Thermal and Light-Induced Spin-Crossover in Salts of the Heptadentate Complex [*Tris*(4-{pyrazol-3-yl}-3-aza-3-butenyl)amine]iron(II)

Hanane Z. Lazar[a], Thibaut Forestier[a], Simon A. Barrett[b], Colin A. Kilner[b], Jean-François Létard*[,a] and Malcolm A. Halcrow*[,b]

[a]*Institut de Chimie de la Matière Condensée de Bordeaux, UPR CNRS 9048 - Université de Bordeaux 1, Groupe des Sciences Moléculaires, 87 Av. Doc. A. Schweitzer, F-33608 Pessac, France. E-mail:letard@icmcb-bordeaux.cnrs.fr*

[b]*School of Chemistry, University of Leeds, Woodhouse Lane, Leeds, UK LS2 9JT. E-mail: m.a.halcrow@leeds.ac.uk*

Electronic Supplementary Information

Table S1 Selected bond lengths and angles (Å, °) for the different crystal structures in this study. Data from $\mathbf{1[ClO_4]_2}\cdot\mathrm{H_2O}$ are taken from ref. 1.

	$\mathbf{1[BF_4]_2}\cdot\mathrm{H_2O}$	$\mathbf{1[ClO_4]_2}\cdot\mathrm{H_2O}$	$\mathbf{1[NO_3]_2}\cdot\mathrm{CH_3NO_2}$					
	150 K	100 K	300 K	250 K	200 K	150 K	100 K	30 K
Fe(1)–N(2)	2.7320(19)	2.7468(17)	2.959(3)	2.966(2)	2.997(3)	3.224(3)	3.433(3)	3.414(8)
Fe(1)–N(5)	2.1509(19)	2.1563(16)	2.184(2)	2.182(2)	2.181(2)	2.085(2)	2.016(3)	2.018(7)
Fe(1)–N(8)	2.2516(19)	2.2547(16)	2.248(3)	2.245(2)	2.223(2)	2.099(2)	2.014(3)	2.023(8)
Fe(1)–N(14)	2.1522(19)	2.1575(17)	2.181(3)	2.180(2)	2.174(2)	2.071(3)	2.008(3)	2.019(9)
Fe(1)–N(17)	2.2531(19)	2.2413(17)	2.240(2)	2.229(2)	2.211(2)	2.098(2)	2.010(3)	2.006(8)
Fe(1)–N(23)	2.1611(19)	2.1628(17)	2.199(3)	2.193(2)	2.178(3)	2.088(2)	2.024(3)	2.028(8)
Fe(1)–N(26)	2.2395(19)	2.2457(16)	2.249(2)	2.240(2)	2.223(2)	2.0957(19)	2.011(2)	2.016(6)
N(2)–Fe(1)–N(5)	67.55(6)	67.23(5)	64.36(9)	64.08(8)	63.36(8)	61.34(8)	59.39(9)	60.0(2)
N(2)–Fe(1)–N(8)	128.54(6)	128.69(5)	124.24(9)	124.01(8)	123.84(8)	123.36(7)	122.58(9)	122.9(2)
N(2)–Fe(1)–N(14)	68.47(6)	68.49(6)	64.70(9)	64.50(8)	64.14(8)	61.25(8)	59.25(9)	59.5(3)
N(2)–Fe(1)–N(17)	126.88(6)	126.82(6)	125.47(9)	125.10(7)	124.87(8)	123.20(7)	122.17(9)	122.6(2)
N(2)–Fe(1)–N(23)	68.25(7)	68.08(6)	64.31(9)	64.19(8)	63.74(8)	61.08(8)	58.99(9)	59.4(2)
N(2)–Fe(1)–N(26)	126.41(6)	126.16(5)	125.21(9)	125.16(7)	124.78(8)	123.73(7)	122.71(9)	122.2(2)
N(5)–Fe(1)–N(8)	74.00(7)	74.02(6)	75.03(10)	74.99(8)	75.52(9)	77.64(8)	79.42(11)	79.3(3)
N(5)–Fe(1)–N(14)	108.70(7)	109.45(6)	102.86(10)	102.67(8)	101.92(9)	99.31(8)	96.68(11)	97.1(3)
N(5)–Fe(1)–N(17)	91.73(7)	92.64(6)	91.70(10)	91.84(8)	91.82(9)	90.90(8)	90.50(11)	90.4(3)
N(5)–Fe(1)–N(23)	105.06(7)	104.25(6)	104.08(10)	103.97(9)	103.25(9)	99.70(9)	96.63(11)	97.3(3)
N(5)–Fe(1)–N(26)	161.02(7)	161.14(6)	165.59(10)	166.02(8)	166.94(8)	169.55(8)	171.48(10)	171.4(3)
N(8)–Fe(1)–N(14)	159.71(7)	159.82(6)	166.09(10)	166.33(8)	166.69(10)	170.28(9)	172.52(11)	172.3(3)
N(8)–Fe(1)–N(17)	86.02(7)	86.13(6)	90.66(10)	91.12(8)	91.20(9)	92.58(8)	93.85(10)	93.4(3)
N(8)–Fe(1)–N(23)	91.17(7)	91.34(6)	92.46(10)	92.67(8)	92.75(9)	92.35(8)	91.72(11)	91.6(3)
N(8)–Fe(1)–N(26)	87.07(7)	87.25(6)	90.64(9)	91.11(8)	91.59(8)	92.40(8)	93.30(10)	93.3(3)
N(14)–Fe(1)–N(17)	73.89(7)	73.95(6)	75.58(10)	75.41(9)	75.75(10)	78.17(9)	79.73(11)	79.7(3)
N(14)–Fe(1)–N(23)	106.99(7)	106.51(6)	101.35(11)	100.93(9)	100.54(10)	97.27(9)	95.09(11)	95.6(3)
N(14)–Fe(1)–N(26)	89.54(7)	88.90(6)	91.41(10)	91.20(8)	91.10(9)	91.02(8)	91.04(11)	90.7(3)
N(17)–Fe(1)–N(23)	161.51(8)	161.53(7)	164.19(9)	164.19(8)	164.93(8)	169.06(8)	171.66(11)	171.4(3)
N(17)–Fe(1)–N(26)	88.29(7)	88.21(6)	89.93(9)	89.93(8)	90.47(9)	92.72(8)	94.44(11)	94.4(3)
N(23)–Fe(1)–N(26)	73.30(7)	73.39(6)	74.54(10)	74.66(8)	74.89(9)	77.32(8)	79.03(11)	78.3(3)

Table S2 Metric parameters for the hydrogen bonds in the crystal structures in this work (Å, °).[a] Data from **$1[ClO_4]_2$**$\cdot H_2O$ are taken from ref. 1.

	D–H	H...A	D...A	D–H...A
$1[BF_4]_2$ $\cdot H_2O$ at 150 K				
N(9)–H(9)…O(40)	0.88	1.99	2.830(3)	159.6
N(18)–H(18)…O(40^{i})	0.88	1.96	2.827(3)	167.5
N(27)–H(27)…F(31A)/F(31B)[b]	0.88	2.00/1.91	2.830(6)/2.766(16)	155.8/165.2
O(40)–H(40A)…F(32A^{ii})/F(32B^{ii})[b]	0.855(15)	1.980(18)/1.79(2)	2.689(3)/2.596(13)	139.5(16)/157.0(19)
O(40)–H(40B)…F(36A)/F(36B)[b]	0.823(16)	2.08(2)/1.88(2)	2.845(14)/2.664(14)	154(2)/158(3)
$1[ClO_4]_2$ $\cdot H_2O$ at 100 K				
N(9)–H(9)…O(40)	0.88	2.00	2.848(2)	160.0
N(18)–H(18)…O(40^{i})	0.88	1.97	2.833(2)	168.1
N(27)–H(27)…O(31)	0.88	2.03	2.848(2)	154.7
O(40)–H(40A)…O(32^{ii})	0.854(19)	2.04(2)	2.728(2)	137.1(16)
O(40)–H(40B)…O(36)	0.84(2)	2.07(2)	2.832(2)	149(2)
$1[NO_3]_2$ $\cdot CH_3NO_2$ at 100 K				
N(9)–H(9)…O(35)	0.88	1.94	2.816(4)	171.4
N(18)–H(18)…O(31)	0.88	1.99	2.865(4)	170.0
N(27)–H(27)…O(33^{iii})	0.88	2.03	2.816(4)	148.6

[a] Symmetry codes: (i) 1–*x*, 1–*y*, 1–*z*; (ii) –1+*x*, *y*, *z*; (iii) ½+*x*, $^{3}/_{2}$–*y*, –*z*. [b] Hydrogen bond to a disordered anion, whose metric parameters should be treated with caution.

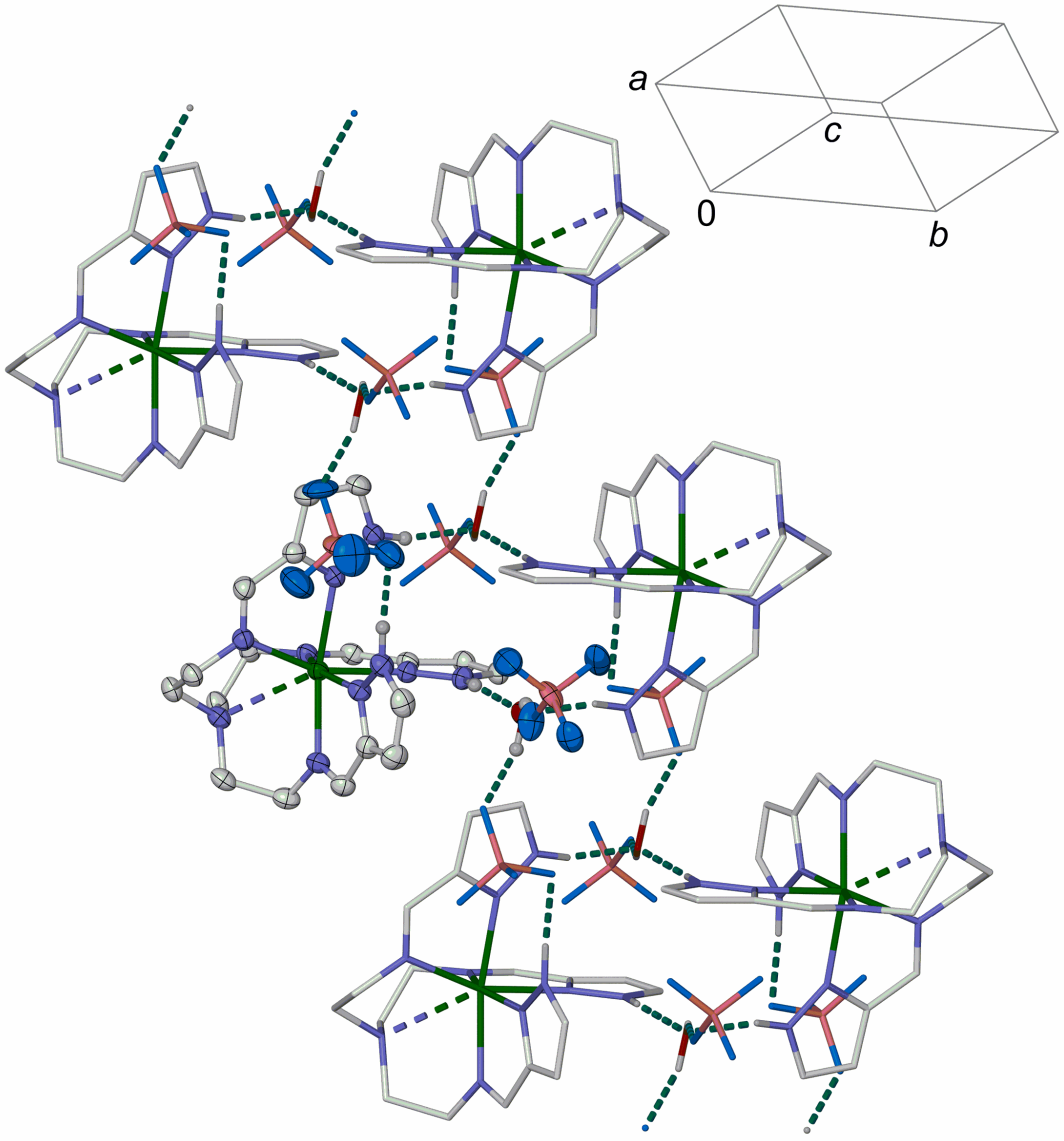

Figure S1 Partial packing diagram of **1[BF$_4$]$_2$**·H$_2$O, showing its association into hydrogen-bonded ladders. The orientation of the unit cell in this arbitrary view is shown in inset (not to scale). The asymmetric unit is plotted with 50% displacement ellipsoids while other atoms have arbitrary radii. For clarity only one orientation of the disordered BF$_4^-$ ions is shown, and all C-bound H atoms have been omitted. Isostructural **1[ClO$_4$]$_2$**·H$_2$O adopts the same packing motif, although its ClO$_4^-$ anions are not disordered.[1] Colour code: C, white; H, grey; B, pink; F, cyan; Fe, green; N, blue; O, red.

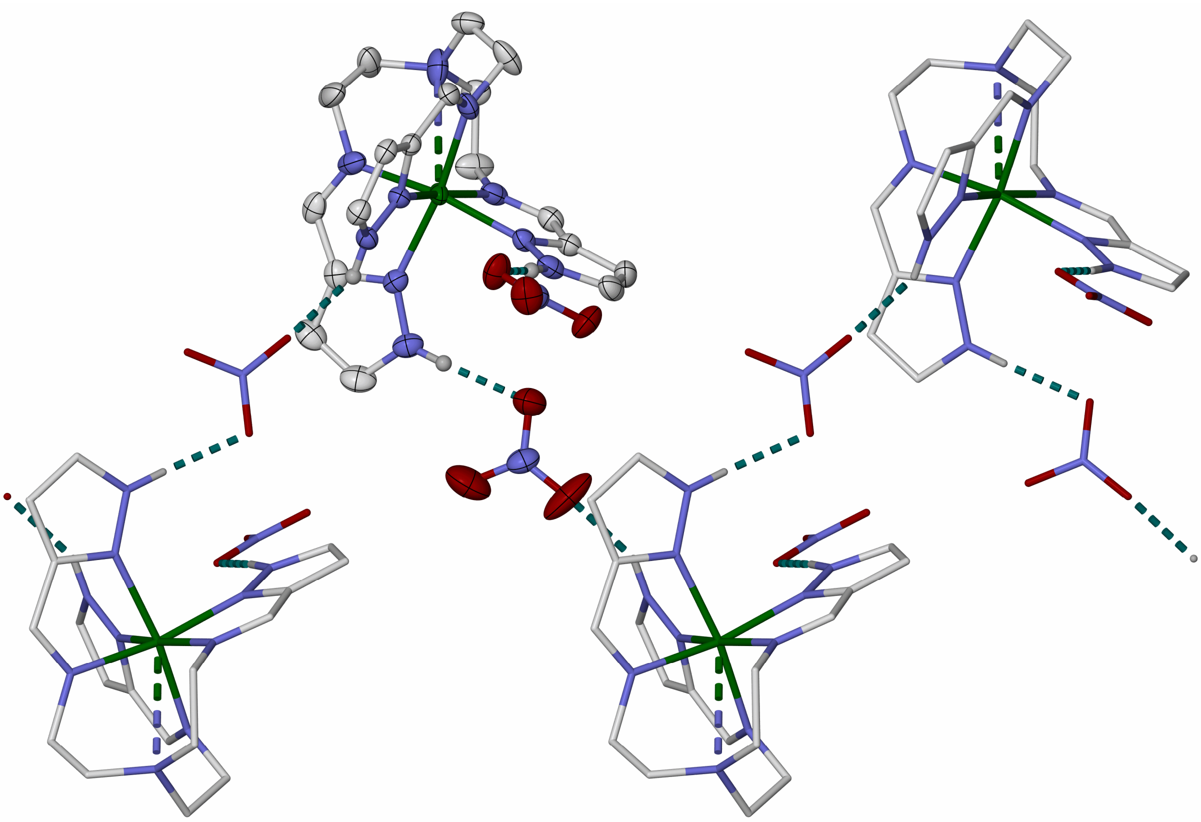

Figure S2 Partial packing diagram of **1[NO$_3$]$_2$**·CH$_3$NO$_2$ at 150 K, showing its association into hydrogen-bonded chains. The view is perpendicular to the (001) crystal plane, with *a* horizontal. The solvent molecules, which do not take part in hydrogen bonding, are not shown. Other details as for Fig. S1.

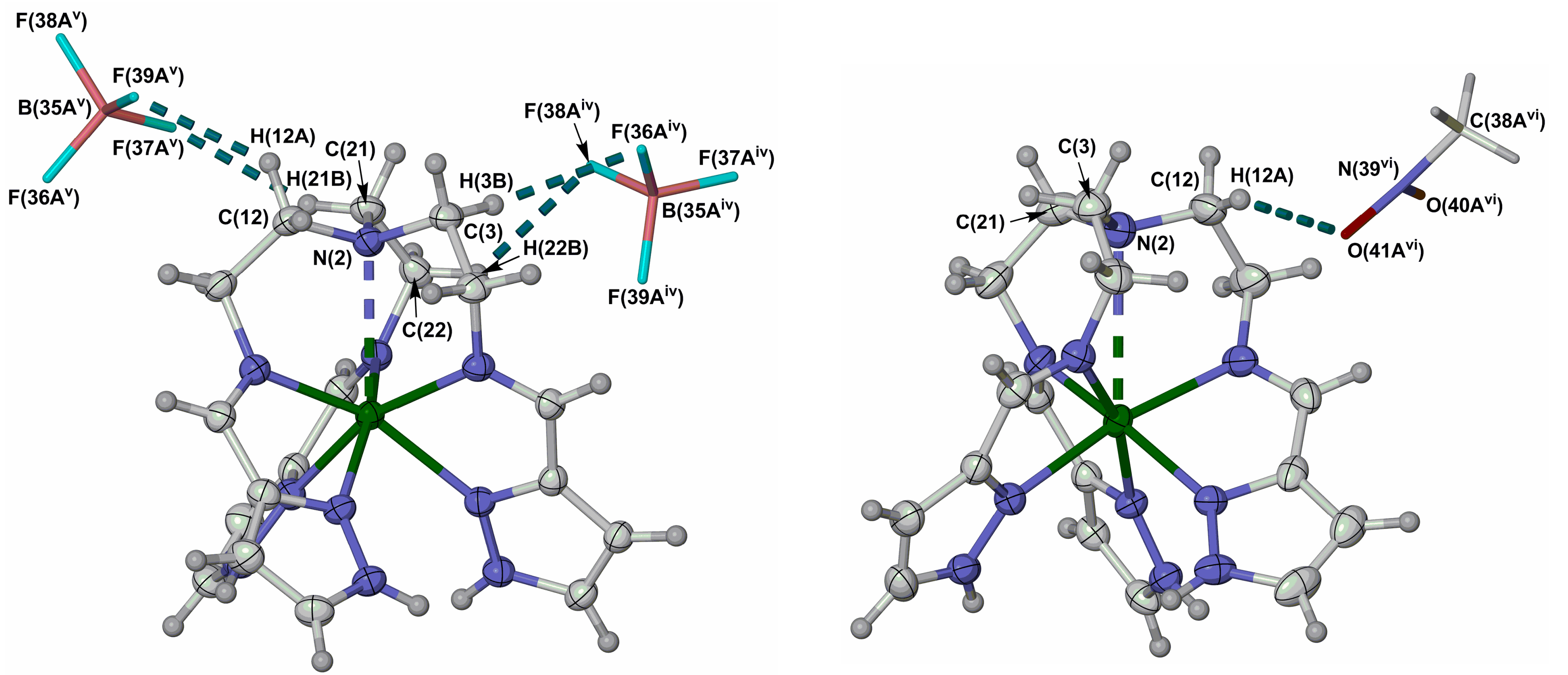

Figure S3 Close intermolecular contacts involving the capping N(CH$_2$)$_3$ moieties in **1[BF$_4$]$_2$**·H$_2$O at 150 K (left) and **1[NO$_3$]$_2$**·CH$_3$NO$_2$ at 200 K (right). Only contacts that are equal to, or closer than, the van der Waals radii of the two interacting atoms are shown. For clarity only one orientation of the disordered BF$_4^-$ ions and CH$_3$NO$_2$ molecule in the structures are shown. Other details as for Fig. S1. Symmetry codes: (iv) ½–*x*, –½+*y*, ½–*z*; (v) 1–*x*, 1–*y*, –*z*; (vi) ½–*x*, 1–*y*, –½+*z*.

Table S3 Metric parameters for the close intermolecular contacts shown in Fig. S3 (Å, °).[a] Since all the interactions listed involve a disordered residue, their metric parameters should be treated with caution. For comparison, the sum of van der Waals radii of a H and F atom is 2.55 Å, and of a H and O atom is 2.6 Å.

	C–H	H...A	C...A	C–H...A
$\mathbf{1[BF_4]_2}\cdot H_2O$ at 150 K				
C(3)–H(3B)…F(36A^{iv})/F(36B^{iv})	0.99	2.55/2.46	3.45(2)/3/38(2)	151.9/153.9
C(12)–H(12A)…F(39A^{v})/F(39B^{v})	0.99	2.40/2.62	3.19(2)/3.37(2)	136.1/132.7
C(21)–H(21B)…F(37A^{v})/F(37B^{v})	0.99	2.50/2.43	3.42(2)/3.52(2)	154.6/156.2
C(22)–H(22B)…F(38A^{iv})/F(38B^{iv})	0.99	2.54/2.67	3.23(2)/3.36(2)	126.6/126.9
$\mathbf{1[NO_3]_2}\cdot CH_3NO_2$ at 200 K				
C(12)–H(12A)…O(41A^{vi})/O(41B^{vi})	0.99	2.42/2.54	3.34(1)/3.39(1)	153.7/144.0

[a] Symmetry codes: (iv) ½–*x*, –½+*y*, ½–*z*; (v) 1–*x*, 1–*y*, –*z*; (vi) ½–*x*, 1–*y*, –½+*z*.

Table S4 Structural parameters for iron(II) complexes of tren-based Schiff base podands (Å, °). Only compounds known to be in a pure spin state at the temperature of measurements are included. See Scheme S1 for the ligands referred to in this Table.

	Fe–N{amine}	av. Fe–N{imine}	av. Fe–N{heterocycle}	Σ	Θ	Spin-crossover on cooling?	Ref
High-spin							
1[BF$_4$]$_2$·H_2O	2.7320(19)	2.155(1)	2.248(1)	111.5(2)	228	No	This work
1[ClO$_4$]$_2$·H_2O	2.7468(16)	2.159(1)	2.247(1)	112.3(2)	229	No	1
$[Fe(L^9)][PF_6]_2$	3.004(8)	2.179(5)	2.219(5)	100.2(12)	241	No	2
$[Fe(L^{10})][NO_3]_2$	3.261(7)	2.182(4)	2.235(4)	83.5(10)	181	No	3
$[Fe(L^{11})][ClO_4]_2$	3.280(3)	2.139(2)	2.322(1)	99.9(3)	203	Not above 80 K	4
1[NO$_3$]$_2$·CH_3NO_2, 300 K	2.959(3)	2.188(2)	2.246(1)	90.1(3)	218	Yes	This work
$[Fe(L^1)][PF_6]_2$	2.753(8)	2.152(6)	2.241(5)	119[a]	n/a	Yes	5
$[Fe(L^5)][BF_6]_2\cdot 3H_2O$, 293 K	2.889(7)	2.195(2)	2.189(2)	103.6(6)	220	Yes	6
$[Fe(L^6)]Cl[I_3]$, 180 K	3.085(4)	2.179(2)	2.211(2)	80.9(5)	195	Yes	7
$[Fe(L^6)]Cl[PF_6]$, 296 K	3.004(3)	2.182(2)	2.220(2)	83.5(3)	192	Yes	8
$[Fe(L^6)]Cl[AsF_6]$, 180 K	2.983(4)	2.176(2)	2.204(2)	83.0(3)	186	Yes	8
$[Fe(L^6)]Cl[SbF_6]$, 180 K	3.017(2)	2.176(1)	2.202(1)	83.8(3)	182	Yes	8
$[Fe(L^6)]Cl[CF_3SO_3]$, 296 K	2.969(2)	2.173(1)	2.231(1)	83.0(3)	192	Yes	8
$[Fe(L^{12})][ClO_4]_2$, 293 K	3.050(3)	2.183(2)	2.193(2)	94.7(5)	229	Yes	9
$[Fe(L^{13})][PF_6]_2$	2.724(4)	2.188(2)	2.246(2)	109.9(7)	219	Not reported	10
$[Fe(L^{13})][ClO_4]_2\cdot CH_3CN$	2.834(3)	2.200(2)	2.216(2)	123.8(3)	260	Not reported	11
Low-spin							
1[NO$_3$]$_2$·CH_3NO_2, 100 K	3.433(1)	2.016(2)	2.012(1)	65.1(4)	154		This work
$[Fe(L^1)][BF_4]_2$	3.439	1.942	1.966	60.3	114		12
$[Fe(L^1)][ClO_4]_2$	3.477(1)	1.948(1)	1.973(1)	61.4(2)	110		13
$[Fe(L^1)][PF_6]_2$	3.435(1)	1.950(2)	1.981(2)	63.9(5)	114		5, 14
$[Fe(L^5)][BF_6]_2\cdot 3H_2O$, 108 K	3.523(2)	1.989(1)	1.981(1)	54.6(5)	139		6
$[Fe(L^6)]Cl[PF_6]$, 93 K[b]	3.376(1)	1.989(2)	1.993(2)	61.1(3)	105		8
$[Fe(L^6)]Cl[AsF_6]$, 90 K	3.372(9)	1.964(5)	1.974(5)	68.3(14)	118		8
$[Fe(L^6)]Cl[SbF_6]$, 90 K	3.350(1)	2.002(1)	2.012(1)	62.6(2)	112		8
$[Fe(L^{14})][ClO_4]_2\cdot H_2O$	3.437(1)	1.980(1)	1.964(1)	59.0(3)	130		15
$[Fe(L^{14})]Cl_{0.5}[PF_6]_{1.5}\cdot 2H_2O$	3.441	1.976	1.959	56.3	128		16
$[Fe(L^{12})][ClO_4]_2$, 100 K	3.527(1)	1.983(1)	1.971(1)	54.3(3)	132		9
$[Fe(L^{15})][ClO_4]_3\cdot 2H_2O$	3.897(1)	1.937(1)	1.955(1)	55.7(5)	133		9
$[Fe(L^{16})][ClO_4]_3\cdot 2H_2O$	3.920(1)	1.951(1)	1.957(1)	54.1(4)	128		9

[a] Estimated value based on incomplete published data. [b] Molecule 2 in the crystal

Table S5 Structural changes during spin-crossover for iron(II) complexes of tren-based Schiff base podands (Å, °). Only compounds for which high- and low-spin crystal structures are listed in Table 1 are included. Data in italics are hypothetical values that **1[BF$_4$]$_2$**·H_2O and **1[ClO$_4$]$_2$**·H_2O would exhibit if they underwent spin-crossover, calculated by comparison with the low-spin structure of **1[NO$_3$]$_2$**·CH_3NO_2. See Scheme S1 for the ligands referred to in this Table.

	Δ*r* Fe–N{amine}	Δ*r* Fe–N{imine}	Δ*r* Fe–N{heterocycle}	ΔΣ	ΔΘ	Ref
1[BF$_4$]$_2$·H_2O	*0.70*	*0.14*	*0.24*	*46*	*74*	This work
1[ClO$_4$]$_2$·H_2O	*0.69*	*0.14*	*0.24*	*47*	*75*	1
1[NO$_3$]$_2$·CH_3NO_2	0.474(4)	0.172(3)	0.234(3)	25.0(5)	64	This work
[Fe(L^1)][PF$_6$]$_2$	0.682(8)	0.202(6)	0.260(5)	55[a]	n/a	5
[Fe(L^5)][BF$_6$]$_2$·3H_2O	0.634(7)	0.206(2)	0.208(2)	49.0(8)	81	6
[Fe(L^6)]Cl[PF$_6$]	0.372(3)	0.193(3)	0.227(3)	22.4(4)	87	8
[Fe(L^6)]Cl[AsF$_6$]	0.39(1)	0.212(5)	0.230(5)	14.7(14)	68	8
[Fe(L^6)]Cl[SbF$_6$]	0.333(2)	0.174(2)	0.190(2)	21.2(4)	70	8
[Fe(L^{12})][ClO$_4$]$_2$	0.477(4)	0.200(2)	0.222(2)	40.4(6)	97	9

[a] Estimated value based on incomplete published data.

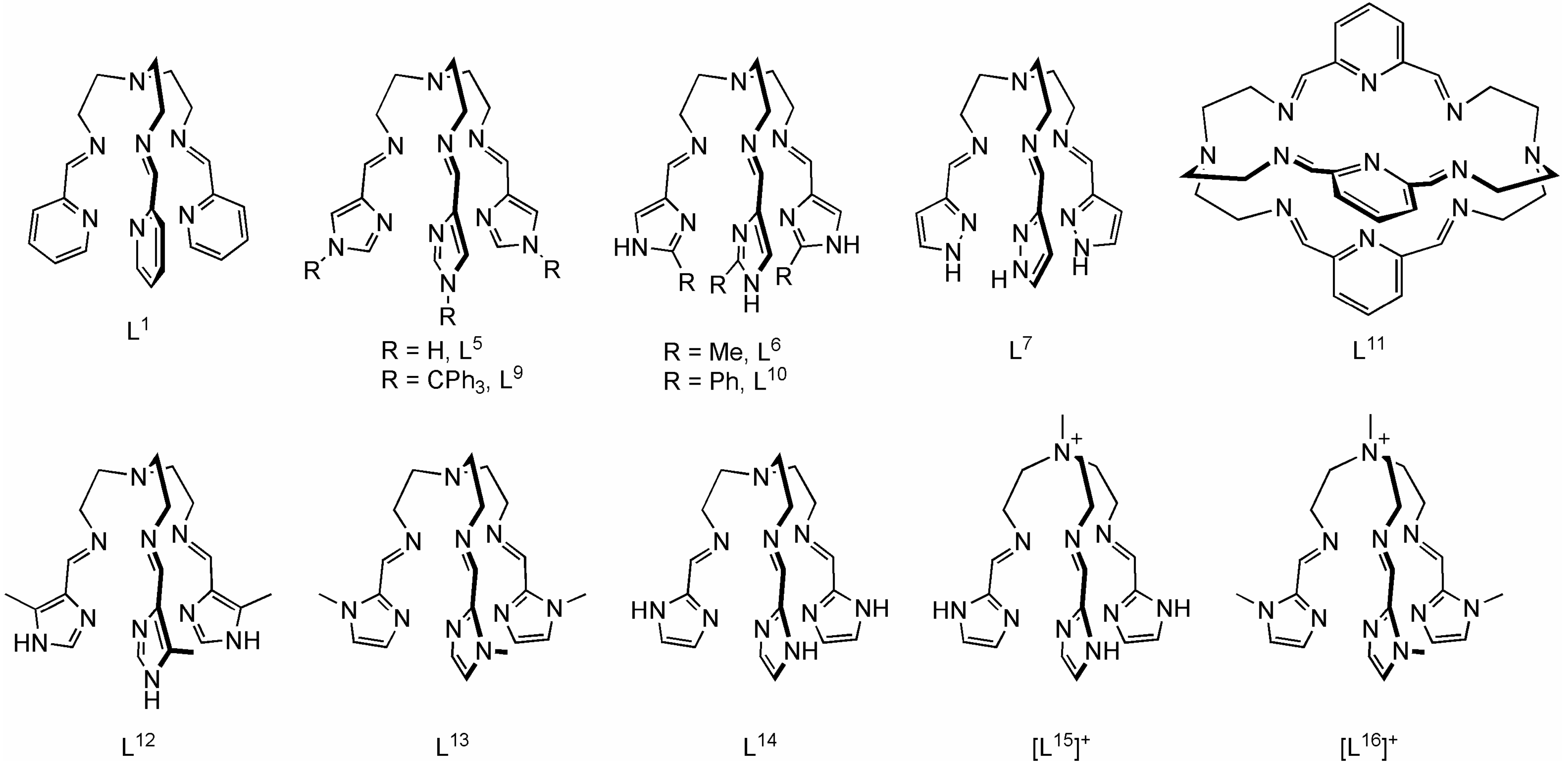

Scheme S1 Ligands referred to in Table S3. L^{1}-L^{7} correspond to the same ligands with those numbers in the main paper.

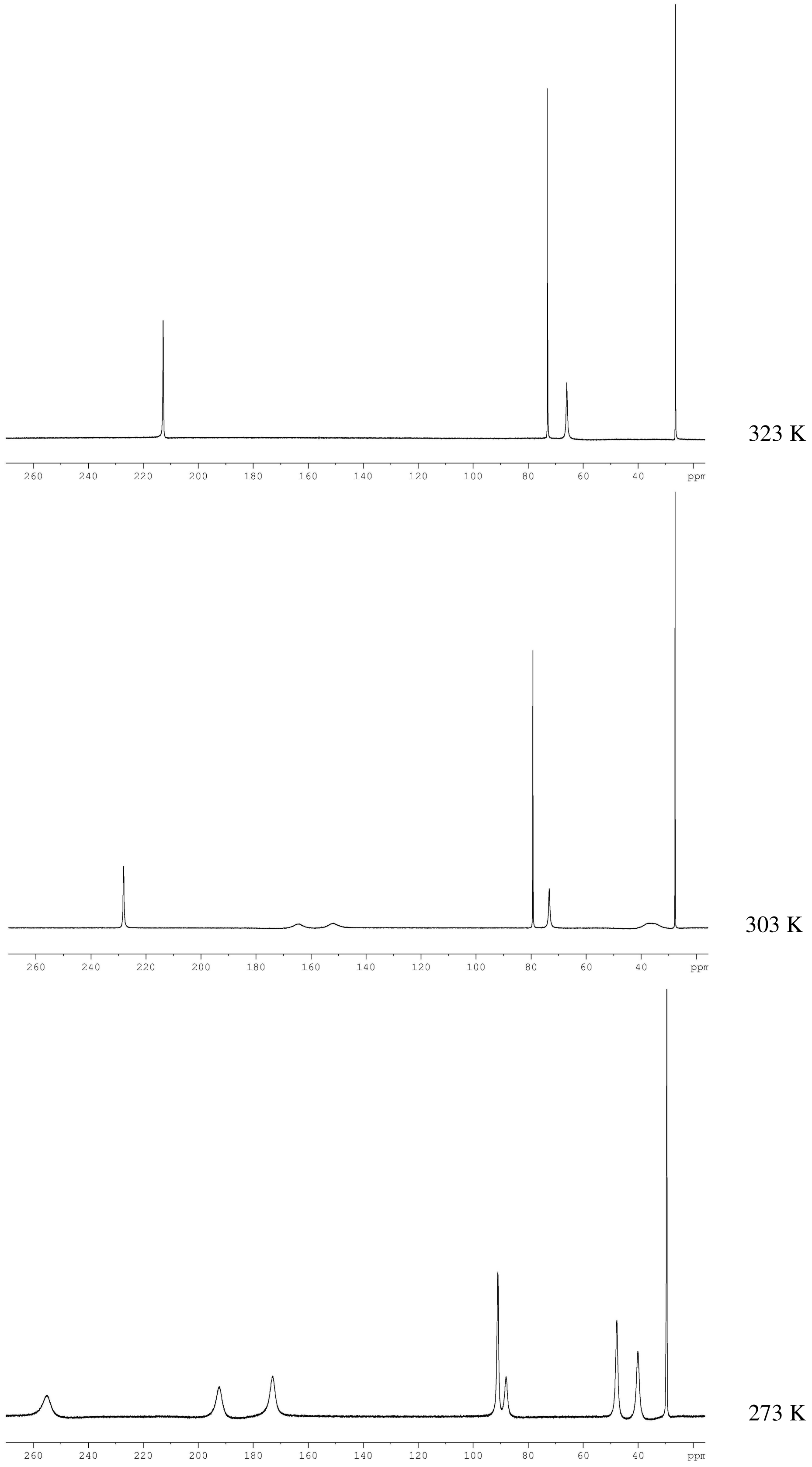

Figure S4 500 MHz ^{1}H NMR spectra of **1[CF$_3$SO$_3$]$_2$** in CD$_3$NO$_2$ at different temperatures, showing the broadening of the peaks from the diastereotopic ligand methylene groups as the temperature is raised. The variation of the contact shifts of the peaks with temperature is normal, and reflects the decreasing susceptibility χ_M of the compound as the temperature is raised. See the main paper for peak assignments.

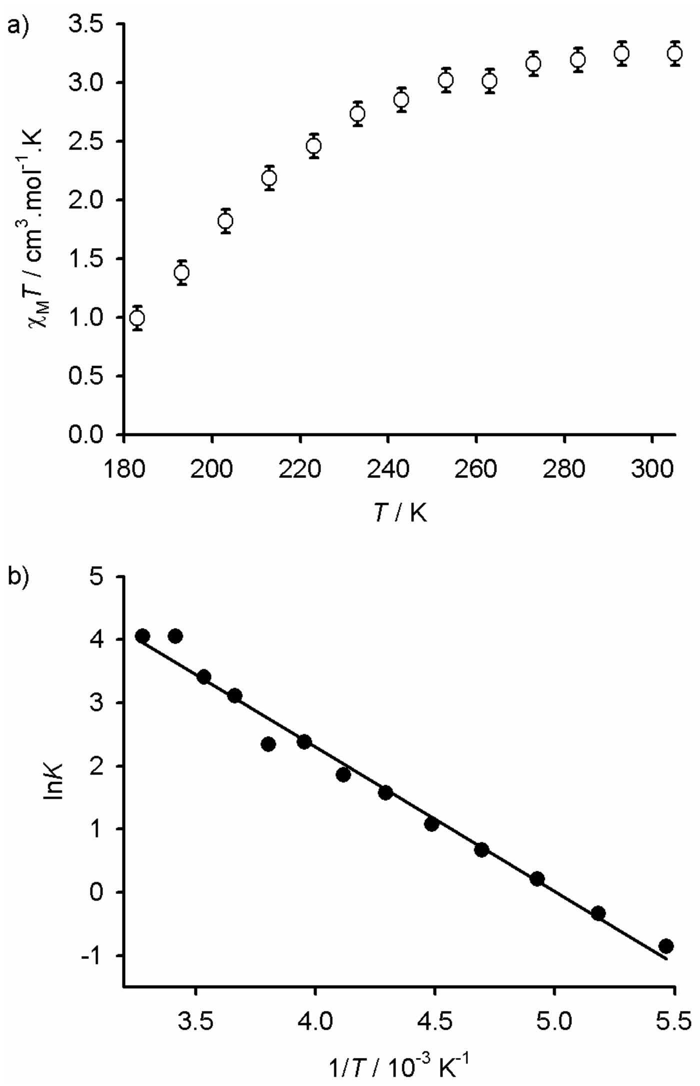

Figure S5 (a) Plot of $\chi_M T$ *vs.* T for **1[CF$_3$SO$_3$]$_2$** in (CD$_3$)$_2$CO. (b) van't Hoff isochore plot of the spin-state equilibrium for **1[CF$_3$SO$_3$]$_2$** from the data in Fig. S5(a), showing the line of best fit.

References

1. M. J. Hardie, C. A. Kilner and M. A. Halcrow, *Acta Cryst.*, 2004, **C60**, m177.

2. I. Morgenstern-Badarau, F. Lambert, A. Deroche, M. Cesario, J. Guilhem, B. Keita and L. Nadjo, *Inorg. Chim. Acta*, 1998, **275-276**, 234.

3. S. Nagasato, I. Katsuki, Y. Motoda, Y. Sunatsuki, N. Matsumoto and M. Kojima, *Inorg. Chem.*, 2001, **40**, 2534.

4. A. F. Deeney, C. J. Harding, G. G. Morgan, V. McKee, J. Nelson, S. J. Teat and W. Clegg, *J. Chem. Soc., Dalton Trans.*, 1998, 1837.

5. I. Morgenstern-Badarau, F. Lambert, J. P. Renault, M. Cesario, J.-D. Marechal and F. Maseras, *Inorg. Chim. Acta*, 2000, **297**, 338.

6. Y. Sunatsuki, H. Ohta, M. Kojima, Y. Ikuta, Y. Goto, N. Matsumoto, S. Iijima, H. Akashi, S. Kaizaki, F. Dahan and J.-P. Tuchagues, *Inorg. Chem.*, 2004, **43**, 4154.

7. M. Yamada, E. Fukumoto, M. Ooidemizu, N. Brefuel, N. Matsumoto, S. Iijima, M. Kojima, N. Re, F. Dahan and J.-P. Tuchagues, *Inorg. Chem.*, 2005, **44**, 6967.

8. M. Yamada, Yamada, H. Hagiwara, H. Torigoe, N. Matsumoto, M. Kojima, F. Dahan, J.-P. Tuchagues, N. Re and S. Iijima, *Chem. Eur. J.*, 2006, **12**, 4536.

9. C. Brewer, G. Brewer, G. Patil, Y. Sun, C. Viragh and R. J. Butcher, *Inorg. Chim. Acta*, 2005, **358**, 3441.

10. S.-P. Yang, Y.-X. Tong, H.-L. Zhu, H. Cao, X.-M. Chen and L.-N. Ji, *Polyhedron*, 2001, **20**, 223.

11. H. M. Chen, S. P. Yang, Q. Q. Chen, J. M. Chen and X. B. Yu, *Acta Cryst.*, 2005, **E61**, m1277.

12. C. Mealli and E. C. Lingafelter, *J. Chem. Soc. D*, 1970, 885.

13. G. Brewer, C. Luckett, L. May, A. M. Beatty and W. R. Scheidt, *Inorg. Chim. Acta*, 2004, **357**, 2390.

14. K. Boubekeur, A. Deroche, F. Lambert and I. Morgenstern-Badarau, *Acta Cryst.*, 1995, **C51**, 2244.

15. C. Brewer, G. Brewer, C. Luckett, G. S. Marbury, C. Viragh, A. M. Beatty and W. R. Scheidt, *Inorg. Chem.*, 2004, **43**, 2402.

16. F. Lambert, C. Policar, S. Durot, M. Cesario, Y. Lu, H. Korri-Youssoufi, B. Keita and L. Nadjo, *Inorg. Chem.,* 2004, **43**, 4178.